Biosensors and Bioelectronics 54 (2014) 165–170

Contents lists available at ScienceDirect

Biosensors and Bioelectronics

journal homepage: www.elsevier.com/locate/bios

An ultrasensitive electrochemical sensing platform for Hg^{2+} based on a density controllable metal-organic hybrid microarray

Lei Shi [a], Zhenyu Chu [a], Yu Liu [a], Wanqin Jin [a,*], Xiaojun Chen [b]

[a] State Key Laboratory of Materials-Oriented Chemical Engineering, College of Chemistry and Chemical Engineering, Nanjing University of Technology, Nanjing 210009, PR China

[b] College of Sciences, Nanjing University of Technology, Nanjing 210009, PR China

ARTICLE INFO

Article history:
Received 7 August 2013
Received in revised form
30 October 2013
Accepted 31 October 2013
Available online 7 November 2013

Keywords:
Metal-organic hybrid microarray
Electrochemical DNA biosensor
DNA cyclic amplification
Nicking endonuclease
Hg^{2+} detection

ABSTRACT

A novel electrochemical Hg^{2+} biosensor was developed on the basis of a metal-organic hybrid microarray, in which the nicking endonuclease (NE) assisted target-triggered strand release strategy was realized *via* the DNA cyclic amplification technique. The metal-organic hybrid microarray was fabricated using the SAM of 1, 4-benzenendithiol as soft template, and the density of the microarray could be adjusted by controlling the surface coverage of 1,4-benzenendithiol molecules. In the presence of Hg^{2+}, capture DNA (cDNA) with an indicator at one end could hybridize with the reporter DNA (rDNA) through the stable T–Hg^{2+}–T linkage, forming the nicking recognition site. After the nicking reaction, the electrochemical indicator dissociated from the electrode surface. The released rDNA and Hg^{2+} could be reused in the sensing system and initiate the next cycle, and more electroactive indicator dissociated from the electrode surface, resulting in a significant signal decrease. The constructed DNA biosensor could detect Hg^{2+} in a wide linear range from 15 pM to 500 nM, with an ultrasensitive detection limit of 5 pM (S/N=3). Furthermore, the biosensor exhibited excellent stability, good reproducibility and high selectivity towards other divalent ions. The proposed sensing system also showed a promising potential for the application in real aquatic product sample analysis.

1. Introduction

Mercuric ions (Hg^{2+}), the ionic style of mercury, are very toxic environmental pollutants, which would affect the immune and nervous systems, alter genetic expression, and cause serious damage to mammals' health even at low concentrations (Morel et al., 1998; Nolan and Lippard, 2008). The upper limit of Hg^{2+} mandated by United States Environmental Protection Agency (EPA) is 2 ppb (10 nM) in drinking water. Therefore, the development of highly sensitive and selective assay methods for determination of Hg^{2+} is of significant importance (Clevenger et al., 1997; Morita et al., 1998; Mor-Piperberg et al., 2010; Liu et al., 2009). Classical methods for Hg^{2+} detection, such as atomic absorption/emission spectroscopy (ABS/AES) (Butler et al., 2006), inductively coupled plasma mass spectrometry (ICP-MS) (Wang et al., 2007), and cold vapor atomic absorption spectroscopy (Bibby and Mercier, 2002) are widely used. However, they generally require expensive and sophisticated instrumentations and thus limit their applications in the routine and effective monitoring of Hg^{2+}. Because of their advantages of simplicity, low cost, portability, and especially feasibility of miniaturization, electrochemical methods, such as differential pulse stripping analysis (Nolan and Kounaves, 1999; Bonfil et al., 2000), chronopotentiometric stripping analysis (Augelli et al., 2005) and quartz crystal microbalance analysis (Ruys et al., 2000), have been developed. However, few methods can meet the requirement of selectivity and sensitivity at the same time, because of the non-specific interaction between the electrode modifier and Hg^{2+} ions.

As the intrinsic and specific interaction between Hg^{2+} and thymine (T), the Tanaka group reported in 2006 that T–T mismatches could selectively capture Hg^{2+} to form T–Hg^{2+}–T base pairs (Tanaka et al., 2006). In contrast, other metal ions, such as Cu^{2+}, Ni^{2+}, Pd^{2+}, Co^{2+}, Mn^{2+}, Zn^{2+}, Pb^{2+}, Cd^{2+}, Mg^{2+}, Ca^{2+}, Fe^{2+} and Ru^{2+}, do not show any notable effect on the stability of T–Hg^{2+}–T DNA duplex (Miyake et al., 2006). This strategy could provide a high selectivity toward environmental Hg^{2+} detection over other related heavy metal ions. More recently, a series of Hg^{2+} DNA biosensors based on T–Hg^{2+}–T are developed. Kong et al. (2009) fabricated an electrochemical label-free biosensor for Hg^{2+} detection with AuNPs-functionalized rDNA as a signal amplifier, which showed a detection limit of 0.5 nM. Park et al. (2012) implemented an electrochemical detection of Hg^{2+} using graphene oxide as the active indicator with a detection limit of 1 nM. In addition, Niu et al. (2011) designed an electrochemical biosensor for

* Corresponding author. Tel.: +86 25 8317 2266; fax: +86 25 8317 2292.
E-mail address: wqjin@njut.edu.cn (W. Jin).

0956-5663/$ - see front matter © 2013 Elsevier B.V. All rights reserved.
http://dx.doi.org/10.1016/j.bios.2013.10.074

Hg^{2+} determination based on target-induced hybridization and the detection limit of 0.6 nM was observed. A most recent report by Zhuang et al. (2013) presented an Hg^{2+} electrochemical biosensor, which used DNA hairpins as recognition elements and exhibited a detection limit of 2.5 nM. It is indicated that all these electrochemical DNA (E-DNA) biosensors could meet the EPA criterion of Hg^{2+} detection in drinking water. However, the Hg^{2+} tends to bio-accumulate in the mammals' body which could gradually accumulate to higher concentrations and eventually cause serious health damage. Therefore, there is an urgent demand to design and develop novel electrochemical biosensors to achieve higher sensitivity for Hg^{2+} detection.

Considerable efforts have been made to develop novel E-DNA biosensor with high sensitivity. Two types of strategies have been investigated towards signal amplification. Firstly, by optimizing the substrate fabrication of E-DNA biosensor, the immobilized amount of cDNA probes was enhanced and the electron transfer was improved (Huang et al., 2009). Secondly, the structure of target identification unit was optimized using DNA hairpins or stem-loop molecular beacons for the detection of targets (Wang et al., 2012; Li et al., 2011; Zhuang et al., 2013), or adopting the rolling circle amplification (RCA), hybridization chain reaction (HCR), polymerase chain reaction (PCR) and ligase chain reaction (LCR) based E-DNA biosensors (Chen et al., 2010; Bi et al., 2013; Choi et al., 2012; Hashimoto et al., 2006). The use of nanomaterials, such as Au or Pt nanoparticles, quantum dots and conductive polymers, as signal amplifiers in the E-DNA biosensors has shown to significantly improve the detection sensitivity (Chen et al., 2008; Wang et al., 2003; Gerard et al., 2002). However, few reports are available about the development of metal-organic hybrid microarray based E-DNA biosensors.

Nuclease signaling amplification (NSA) has been reported as a new method for amplified DNA/target detection, which is based on DNA/target recycling amplification with the assistance of various nucleases, including endonucleases and exonucleases (Chen et al., 2010; Tong et al., 2011). Various nucleases can lead to direct recycling and reuse of DNA/target, which in turn results in substantial signal amplification for DNA/target determination. In particular, the nucleases reactions can be performed in an isothermal condition without sophisticated instrumentation and therefore have wide applications in routine bioanalysis.

Herein, we described an E-DNA biosensor for Hg^{2+} detection based on a metal-organic hybrid microarray coupling the NE assisted target-induced strand release strategy. Highly oriented hybrid microarray of $Ni(en)_3Ag_2I_4$ (where en represents diaminoethane) was fabricated by a facile and reliable method based on the 1,4-benzenendithiol modified Au substrate through the Ag–S covalent interaction. In addition, the density of the microarray could be controlled by adjusting the distribution of the 1,4-benzenendithiol layer. The 5′–SH modified stem-loop structured cDNA molecules were immobilized onto the $Ni(en)_3Ag_2I_4$ microarray surface by Ag–S bonding. The electroactive 3′-methylene blue (MB) probe approaching the electrode surface resulted in an obvious current signal. The rDNA with four T–T mismatches could not hybridize with the cDNA on the electrode surface in the absence of Hg^{2+}. However, in the presence of Hg^{2+}, they could hybridize through T–Hg^{2+}–T coordination chemistry. Following the hybridization, the nicking recognition site formed and triggered the nicking reaction. After several cycles, indicator molecules dissociated from the electrode surface and led to the decrease in the peak current of MB, which could be used for the electrochemical quantitative determination of Hg^{2+}. The detection limit of this biosensor using this method was 5 pM, which reached the EPA limit of Hg^{2+}. In addition, the proposed method was also applied to the determination in real aquatic environmental samples.

2. Experimental section

2.1. Chemicals and materials

The NE (Nb.BtsI) was obtained from New England Biolabs. All oligonucleotides were synthesized by TaKaRa biotechnology Co., Ltd. (Dalian, China), and their base sequences were as follows: cDNA: 5′-SH-$(CH_2)_6$-GGT ACG CAG **CTC TTC TC↓C ACT GC**G TAC C-3′-methylene blue (the **CTCTTCT** sequence represents the Hg^{2+} binding sites; the **CGTCAC** sequence is the recognition sequence of NE, and the arrow indicates the nicking position), rDNA: 5′-CGT GAC GTT GTG TT-3′. Ethylenediaminetetraacetic acid (EDTA), 1,4-benzenendithiol, hexaammineruthenium (III) chloride (RuHex, 98%), tris (2-carboxyethyl) phosphine hydrochloride (TCEP), potassium ferricyanide ($K_3Fe(CN)_6$) and potassium ferrocyanide ($K_4Fe(CN)_6$) were purchased from Sigma-Aldrich. $AgNO_3$, KI, N, N-dimethylformamide (DMF), 1,2-ethylenediamine, KCl, NaCl, NaH_2PO_4, Na_2HPO_4, $HgCl_2$, $CoCl_2$, $ZnCl_2$, $MgCl_2$, $CaCl_2$, $Pb(NO_3)_2$, $MnCl_2$, $CuSO_4$, $Ni(NO_3)_2$, $Ba(NO_3)_2$ and $CdCl_2$ were obtained from Sinopharm Chemical Reagent Co., Ltd. All solutions were made up using ultrapure water of resistivity ~18.2 MΩ cm (Millipore, MA). Aqueous environmental samples in Taihu Lake (Soochow) containing Hg^{2+} were obtained from Entry-exit Inspection and Quarantine Bureau, Jiang Su Province, China.

2.2. Buffers

Immobilization buffer (I-buffer): 10 mM Tris–HCl + 1 mM EDTA + 0.1 M NaCl + 10 mM TCEP + 10 mM $MgCl_2$ · (pH 7.4), Mg^{2+} was added into the I-buffer to induce the formation of the stem-loop structure of DNA probes. Hybridization buffer (H-buffer): 10 mM phosphate buffer + 0.25 M NaCl (pH 7.4). Washing buffer (W-buffer): 10 mM Tris–HCl (pH 7.4). NE buffer: 20 mM Tris-acetate + 50 mM potassium acetate + 10 mM magnesium acetate + 1 mM dithiothreitol (pH 7.9).

2.3. Formation of $Ni(en)_3Ag_2I_4$ microarray modified Au substrate

The diameter of the Au substrate was controlled by the insulating tape and determined to be 1 mm. The Au substrate was pretreated following the known procedure (Zhang et al., 2007). The freshly cleaned Au substrate was immersed in the 5 mM 1,4-benzenendithiol ethanol solution for different time from 2 to 10 h to form the SAM structure and was then sufficiently rinsed with ethanol. Hybrid mother solution of $Ni(en)_3Ag_2I_4$ was prepared as described previously (Jiang et al., 2008, Shi et al., 2013a). Here special treatment was needed: the mother solution was maintained at 80 °C for 72 h, then heated to 100 °C and kept for 24 h, and finally slowly cooled to 25 °C. The sediment formed during the treatment procedure was removed from the hybrid mother solution with a filter membrane. The $Ni(en)_3Ag_2I_4$ microarray modified Au substrate was then fabricated by vertically dipping the Au substrate into the solution to crystallize at 25 °C for 10 h. For comparison, disordered $Ni(en)_3Ag_2I_4$ hybrid film modified Au electrode was prepared using the similar method but without 1,4-benzenendithiol SAM template.

2.4. DNA immobilization, hybridization and the nicking reaction

Firstly, the $Ni(en)_3Ag_2I_4$/Au was incubated into a 2 μM cDNA solution at 37 °C for 5 h in 100% humidity. The electrode was thoroughly rinsed with W-buffer to reduce the physical adsorption of cDNA and further incubated in the hybridization solution containing 1 μM rDNA and Hg^{2+} with various concentrations for 2 h at room temperature. After hybridization, the electrode was thoroughly rinsed with W-buffer and dried under a stream of

nitrogen gas. The electrode was then incubated in a solution of NE (10 U/μL) in NE Buffer supplemented with 100 μg/mL bovine serum albumin (BSA) at 37 °C. After a specific period of 2 h, the electrode was rinsed with W-buffer and used for the performance tests.

2.5. Electrochemical measurements

All electrochemical experiments were performed with a CHI 660C electrochemical workstation (Shanghai CH, China). A conventional three-electrode configuration was employed during the experiment, which involved a $Ni(en)_3Ag_2I_4$/Au working electrode, a platinum auxiliary electrode, and an Ag/AgCl (sat. KCl) reference electrode. Cyclic voltammetry (CV) was carried out at different scan rates, square wave voltammetric (SWV) measurements were taken at a frequency of 5 Hz, electrochemical impedance spectroscopy (EIS) measurements were performed with the frequency changed from 0.01 Hz to 100 kHz with signal amplitude of 5 mV and chronocoulometry (CC) measurements were conducted at a pulse width of 0.25 s. The electrolytes for CV and SWV was 10 mM phosphate buffer and 0.25 M NaCl (pH 7.4), for CC was 10 mM Tris–HCl (pH 7.4) and for EIS was 5 mM $K_3[Fe(CN)_6]/K_4[Fe(CN)_6]$ and 0.1 M KCl solution. Nitrogen atmosphere was maintained throughout the CC measurement.

3. Results and discussion

3.1. Formation of hybrid microarray

The hybrid material, with a formula of $Ni(en)_3Ag_2I_4$, was displayed in Fig. S1. The unique framework of $\{Ag_2I_4^{2-}\}_\infty$ structure imparts some novel properties of photons and electronics to this hybrid material. Here, the formation mechanism of the hybrid films was also proposed, which might involve the structure-directing power between the assembled 1,4-benzenendithiol SAM and the hybrid crystals, as shown in Fig. S2. The electrical conductivity of a single crystal was examined using the four-probe method (Fig. S3) and the conductivity of 8.9×10^{-4} S cm^{-1} was obtained at the room temperature (Yang et al., 2010). Although the conductivity of the hybrid material was not so excellent compared with some metal conductors, e.g. the bulk gold with a high conductivity of about 4.1×10^5 S cm^{-1}, the hybrid microarray could provide enhanced surface area and endow some special properties, which could increase the immobilized amount of cDNA, enhance the diffusion profile, facilitate the mass transfer and thus improve the performance in the Hg^{2+} assay. In addition, this material shows high chemical stability in a phosphate buffer saline (PBS) (pH = 6.8–7.8) and robust resistance to ambient illumination compared with silver iodide.

Au substrate for the growth of hybrid microarray was modified with 5 mM 1,4-benzenendithiol ethanol solution to create an artificial SAM. One terminal –SH group of the SAM was anchored onto the surface of the Au substrate *via* an Au–S bond, the other terminal –SH group was expected to bind with Ag ions of the hybrid crystal. As shown in Fig. 1A, the highly integrated and homogeneous hybrid microarray, consisting of the hexagonal prism-shaped crystals with an average side length of ca. 5 μm, was obtained on the Au substrate. For this oriented hexagonal prism-shaped microarray, only two Bragg reflections indexed as (002) and (004) appeared in the XRD profile (Fig. 1C), indicating that the hybrid microarray grew on the 1,4-benzenendithiol SAM was highly oriented along the crystallographic [001] direction. Bare Au substrate without 1,4-benzenendithiol SAM was also served for the growth of hybrid films, as shown in Fig. 1B, in contrast, the disordered hybrid microcrystals were obtained on the bare Au substrates with various sizes of single crystal, and the XRD showed no uniform crystallographic orientation under this condition (Fig. 1D).

In addition, the effect of different surface coverage of 1, 4-benzenendithiol molecules on the morphologies of hybrid microarray was investigated. As the Au substrate was immersed in the 5 mM 1,4-benzenendithiol ethanol solution for various time, the density of hybrid microarray changed accordingly (Fig. S4).

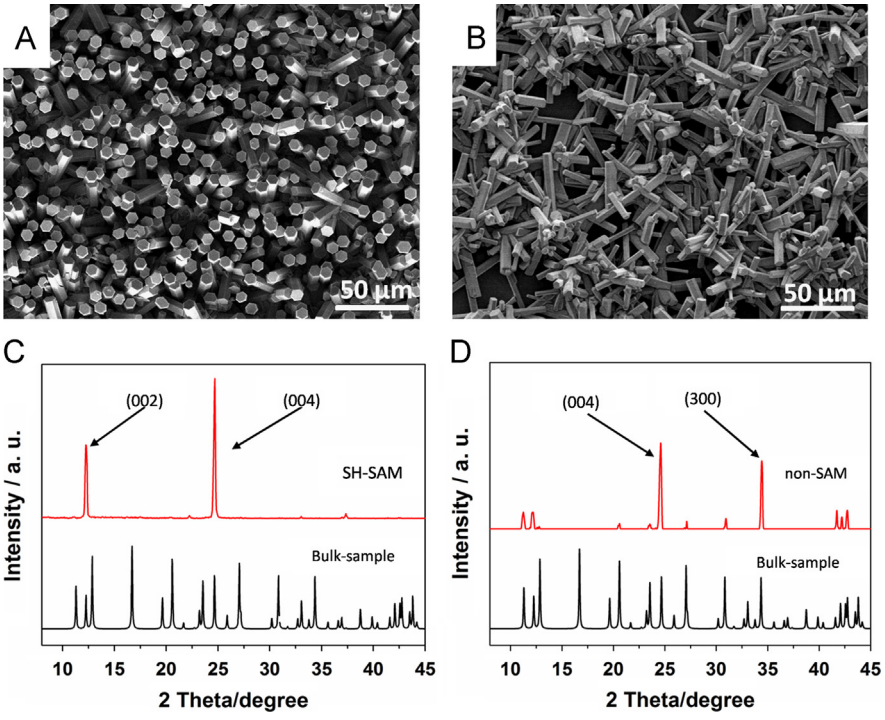

Fig. 1. (A) and (B) FESEM images of hybrid films with different morphologies grown on the 1,4-benzenendithiol SAM modified Au substrate and bare Au substrate respectively. (C) and (D) X-ray diffraction patterns corresponding to (A) and (B).

A sparse microarray was obtained when the assembled time was short; while a crowded microarray was observed under a longer assembled time. For appropriate assembled time of 6 h, homogenous microarray was prepared with each microcrystal separated at a proper distance. Also, CV was applied to characterize the electrochemical performance of these obtained hybrid films modified electrodes in a 10 mM $K_3Fe(CN)_6$ containing 3 M KCl solution at a scan rate of 100 mV s^{-1} (Shi et al., 2013b). As shown in Fig. S5, the highest peak current was observed on the microarray with the modification time of 6 h in 1,4-benzenendithiol, suggesting that this ordered hybrid microarray possessed the largest effective surface area and the highest conductivity. Shorter or longer modification time would make the microarray sparser or denser, leading to the decline of peak currents (Fig. S5B). Therefore, the modification time of 6 h was selected throughout our work.

3.2. Design of the Hg^{2+} detection strategy

The fabrication process of the developed sensitive Hg^{2+} biosensor was illustrated in Fig. 2. The sequences of Hg^{2+} binding sites and NE recognition sites are embedded into the cDNA containing a thiol group at the 5′ end and a MB tag at the 3′ end. The cDNA was covalently attached to the microarray modified electrode through Ag–S bonding. In the absence of Hg^{2+}, few rDNA molecules might physically adsorb onto the electrode surface and the stem-loop structure of most cDNA kept unchanged, resulting in a slight change in the current signal of MB. In contrast, stable base pairs of T–Hg^{2+}–T would form in the presence of Hg^{2+}, then the rDNA could perfectly match with the cDNA and the nicking reaction would happen afterwards. Thus, the cDNA was cleaved into two segments and the MB labeled segment dissociated from the electrode surface, leading to the distinct decrease in the electrochemical response of MB. Furthermore, the released rDNA and Hg^{2+} could be used in the cleavage cycle again, and the further dissociated MB labeled segments enhanced the signal decrease.

3.3. Electrochemical characterizations of designed Hg^{2+} biosensor

To demonstrate the design, the electrochemical behavior of MB in different steps was investigated by CVs, as shown in Fig. 3. Initially, the MB tag contained in the stem-loop structure of cDNA was close to the electrode surface, causing a large current response and a small peak separation (ΔE) of 50 mV (curve a in Fig. 3A). After cDNA hybridized with the rDNA in the presence of Hg^{2+}, stand-up duplex DNA strands were formed, leading the MB tag away from the electrode surface. The current signal declined significantly and the ΔE increased to 140 mV (curve b in Fig. 3A). In the presence of NE, some of the MB tags dissociated from the electrode surface because of the nicking reaction, resulting in a much lower current signal, as shown in curve c of Fig. 3A. In contrast, the hybridization process in the absence of Hg^{2+} showed

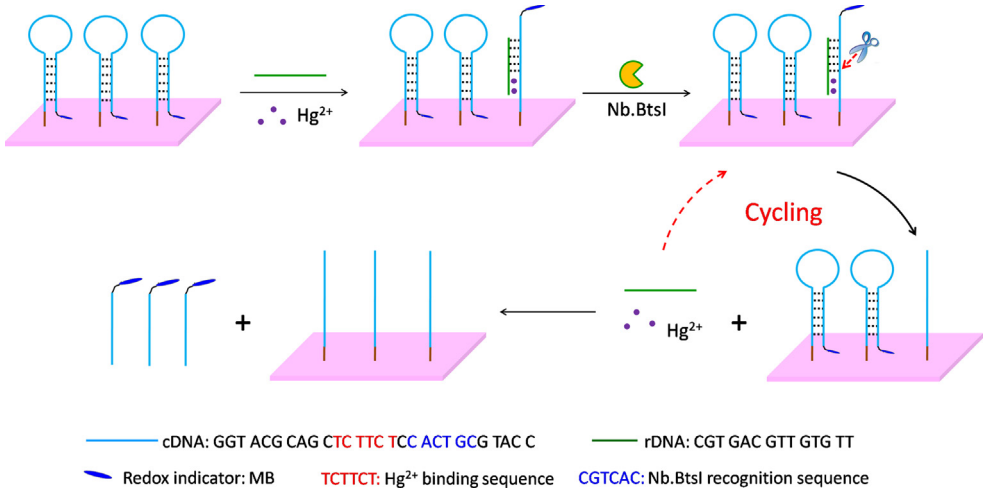

Fig. 2. Schematic illustration of the electrochemical Hg^{2+} sensing strategy coupling with the NE reaction.

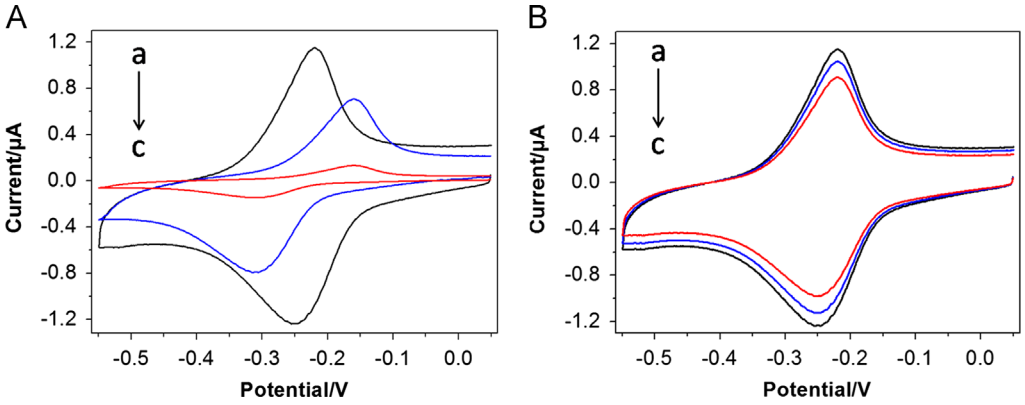

Fig. 3. CVs in the PBS solution of the Hg^{2+} biosensor at different sensing procedures (A) in the presence of 5 nM Hg^{2+}, (B) in the absence of Hg^{2+}: (a) before, (b) after hybridizing with the rDNA and (c) after the nicking reaction. Scan rate of CV was 0.1 V s^{-1}.

slight signal changes in CV curves, indicating that the hybridization and nicking reaction could not be activated without Hg^{2+} (Fig. 3B). Additionally, the EIS measurements were also implemented to monitor the impedance changes during the hybridization process and the result was consistent with that in CVs, as shown in Fig. S6. The target induced strand release strategy was expected to give a larger signal change magnitude than the target induced conformational change, in which the electrochemical events were usually recorded based on the distance alteration between the redox species and the electrode surface. Moreover, in the presence of more amount of Hg^{2+}, the larger signal changes resulted in an enhanced sensitivity.

3.4. Optimization of the experimental conditions

Chronocoulometry was implemented to estimate the surface density (Γ_{ss}) of cDNA immobilized on the electrode surface, using RuHex as electrochemical probe (Steel et al., 1998). The redox charge (Q) of RuHex was proportional to the amount of cDNA which was depended on the incubation time in cDNA solution. With the incubation time increasing from 1 to 9 h, the Γ_{ss} value increased from 2.3×10^{11} to 5.6×10^{12} molecules/cm^2, as shown in Fig. S7A. Furthermore, the effect of the incubation time of cDNA on the performances in the Hg^{2+} assay was investigated. With an Hg^{2+} concentration of 10 nM, it could be seen from Fig. S7B that the current change signal (Δi) increased with the incubation time ranged from 1 h to 5 h. After that, the value of Δi decreased sharply along with the prolonged incubation time. As expected, the low surface density of cDNA usually resulted in weak signals, while the Hg^{2+}-mediated hybridization of cDNA and rDNA, as well as the nicking efficiency was hindered in a high distribution density of cDNA (Lao et al., 2005; Zhang et al., 2006). Therefore, the incubation time of 5 h was adopted in this work, corresponding to the Γ_{ss} value of 1.2×10^{12} molecules/cm^2. Meanwhile, as the poisonous Hg^{2+} may disturb the activity of NE, the dosage of the NE was investigated. As shown in Fig. S8, a dosage of 20 U NE was proved to be adequate and efficient to realize the desired nicking reaction in the Hg^{2+} assay. Furthermore, the time for the nicking reaction was also optimized here. Although the NE possessed high activity in proper conditions, the nicking rate would be restricted at low concentration of Hg^{2+}, since at that time only small amount of duplex DNA strands could be formed. It was obvious that the reaction rate was dependent on the concentration of Hg^{2+} and a more rapid rate was observed with a higher Hg^{2+} concentration (Fig. S9). Considering different reaction rates under various Hg^{2+} concentrations, the reaction time was optimized as 2 h for all the assays in this work.

3.5. Sensitivity of the Hg^{2+} biosensor

The sensitivity of the electrochemical biosensor for the detection of the Hg^{2+} was further investigated by varying the Hg^{2+} concentrations, and SWV was applied to monitor the Δi. It was obviously seen that the current signal of MB tag decreased with the increase of Hg^{2+} concentrations from 0 pM to 2 μM, owing to the more MB tags left the electrode surface when more Hg^{2+} was introduced into sensing system (Fig. 4A). The linear relationship between Δi and the logarithm of the Hg^{2+} concentration was obtained in the range of 15 pM to 500 nM (Fig. 4B) with a sensitive detection limit of 5 pM (S/N=3). Although it was found that a reaction time of 4 h was needed in our assay, which was a little longer than most Hg^{2+} sensors (shown in Table S1), the performance of the prepared Hg^{2+} biosensor was better than that of previous reported T–Hg^{2+}–T based biosensors and some ASV sensors (Kong et al., 2009; Park et al., 2012; Niu et al., 2011; Zhuang et al., 2013; Yuan et al., 2011; Wang et al., 2012; Nolan and Kounaves, 1999; Bonfil et al., 2000). In addition, the performance of Hg^{2+} biosensor based on the disordered hybrid film was also investigated for comparison. As shown in Fig. S10, a higher detection limit of 4 nM (S/N=3), as well as smaller signal responses was observed. It was estimated that the disordered hybrid films possessed smaller surface area, and the cluttered surface structure would reduce the effective immobilization sites for cDNA, which might in turn influence the hybridization with rDNA and disturb the current signal recognition.

3.6. Selectivity of the Hg^{2+} biosensor

The selectivity of the as-prepared biosensor for Hg^{2+} was investigated by monitoring the Δi value after adding other familiar divalent metal ions, e.g. Co^{2+}, Zn^{2+}, Mg^{2+}, Ca^{2+}, Pb^{2+}, Mn^{2+}, Cu^{2+}, Ni^{2+} and Cd^{2+}. The 1 nM Hg^{2+}, 1 mM interesting metal ions and the mixture of 1 nM of Hg^{2+} and 1 mM of all other metal ions were added into the hybridization solution, respectively. As shown in Fig. 5, the biosensor showed an almost neglectable response to other metal ions of 1 mM compared with that from Hg^{2+} at 1 nM. The results demonstrated that the biosensor possessed excellent selectivity for Hg^{2+} over other metal ions, due to the highly specific interaction of T–Hg^{2+}–T coordination.

3.7. Practical application of the Hg^{2+} biosensor

Owing to the excellent selectivity of our proposed biosensor, the application in the detection of Hg^{2+} concentration in environmental samples was demonstrated for the aquatic samples. The samples were measured by both our biosensor and commercial ICP-MS

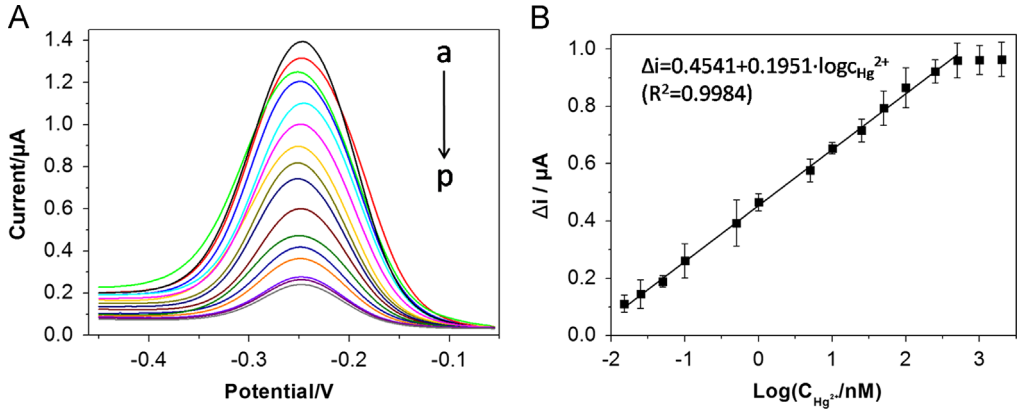

Fig. 4. (A) SWV responses of the Hg^{2+} biosensor after the addition of different concentrations of Hg^{2+} ions (from a to p were 0 pM, 15 pM, 25 pM, 50 pM, 100 pM, 0.5 nM, 1 nM, 5 nM, 10 nM, 25 nM, 50 nM, 100 nM, 250 nM, 500 nM, 1 μM and 2 μM, respectively). (B) Calibration relationship of Δi with logarithm of the Hg^{2+} concentration.

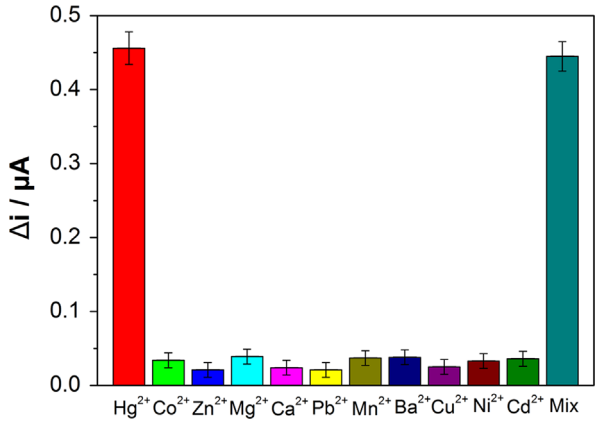

Fig. 5. SWV signal changes (Δi) for the biosensor after being treated with 1 nM of Hg^{2+}, 1 mM of other divalent metal ions, and mixtures of 1 nM of Hg^{2+} with 1 mM of other metal ions.

Table 1
Determination of Hg^{2+} from aquatic product extraction samples using as-prepared biosensor and ICP-MS.

Sample	ICP-MS/nM	Proposed biosensor/nM[a]	Recovery/%
1	0.10	0.11 ± 0.02	110
2	0.50	0.52 ± 0.04	104
3	1.00	0.98 ± 0.07	98
4	10.00	9.97 ± 0.12	99.7
5	30.00	29.85 ± 0.14	99.5

[a] Mean of three measurements ± standard deviation.

method, and the results were listed in Table 1. Both the mean concentration and recovery determined by our biosensor were in good agreement with ICP-MS results, which confirmed that the proposed biosensor can be used for environmental detection and monitoring of Hg^{2+}, even of very low concentrations.

3.8. *Stability and reproducibility of the Hg^{2+} biosensor*

The stability and reproducibility of Hg^{2+} biosensor are extremely important for the practical applications. The cDNA modified electrodes were firstly stored in the refrigerator at 4 °C for 1 week, 2 weeks and 3 weeks respectively, and then used for the measurements of Hg^{2+}. The results demonstrated that the fabricated biosensor retained about 91% of its initial response even after 3 weeks (Fig. S11A). In addition, the reproducibility was also investigated. Five independent experiments were carried with different electrodes, and the results showed that no significant changes in current response were observed (Fig. S11B).

4. Conclusions

In this paper, we have developed an ultrasensitive E-DNA biosensor for the amplified analysis of Hg^{2+} based on a density-controllable metal-organic hybrid microarray. Herein we demonstrated the proof of concept method that the Hg^{2+} biosensor can sensitively and selectively detect Hg^{2+} in the real environmental samples. The assay has several excellent features. Firstly, the metal-organic hybrid microarray was fabricated using 1,4-benzenendithiol SAM as soft template, by which the surface coverage was controllable. Secondly, the introduction of NE induced the cycling amplified detection of target Hg^{2+}, which greatly improved the sensitivity. Thirdly, it possessed high specificity and stability. The detection limit obtained for Hg^{2+} was 5 pM, which were 3 orders of magnitude lower than that of the disordered hybrid film modified electrode. Finally, this system showed a new promising method for designing the cyclic amplification strategy in the application of E-DNA biosensors.

Acknowledgments

This work was supported by the National Natural Science Foundation of China (Nos. 21176115 and 20905035), Doctoral Fund of Ministry of Education of China (20113221110001), Innovation Foundation for Doctoral Dissertation of Jiangsu Province (CXLX12_0443) and State Key Laboratory of Materials-Oriented Chemical Engineering (KL10-15).

Appendix A. Supplementary material

Supplementary data associated with this article can be found in the online version at http://dx.doi.org/10.1016/j.bios.2013.10.074.

References

Augelli, M.A., Munoz, R.A.A, Richter, E.M., Gouveia, A., Angnes, L., 2005. Electroanalysis 17, 755–761.
Bi, S., Zhao, T.T., Luo, B.Y., Zhu, J.J., 2013. Chem. Commun. 49, 6906–6908.
Bibby, A., Mercier, L., 2002. Chem. Mater. 14, 1591–1597.
Bonfil, Y., Brand, Y., Kirowa-Eisner, E., 2000. Anal. Chim. Acta. 424, 65–76.
Butler, O.T., Cook, J.M., Harrington, C.F., Hill, S.J., Rieuwerts, J., Miles, D.L., 2006. J. Anal. At. Spectrom. 21, 217–243.
Chen, J., Zhang, J., Li, J., Fu, F., Yang, H.H., Chen, G., 2010. Chem. Commun. 46, 5939–5941.
Chen, X., Wang, Y., Zhou, J., Yan, W., Li, X., Zhu, J.J., 2008. Anal. Chem. 80, 2133–2140.
Choi, J.Y., Kim, Y.T., Ahn, J., Kim, K.S., Gweon, D.G., Seo, T.S., 2012. Biosens. Bioelectron. 35, 327–334.
Clevenger, W.L., Smith, B.W., Winefordner, J.D., 1997. Crit. Rev. Anal. Chem. 27, 1–26.
Gerard, M., Chaubey, A., Malhotra, B.D., 2002. Biosens. Bioelectron. 17, 345–359.
Hashimoto, M., Barany, F., Soper, S.A., 2006. Biosens. Bioelectron. 21, 1915–1923.
Huang, X.J., O'Mahony, A.M., Compton, R.G., 2009. Small 5, 776–788.
Jiang, Y.S., Yao, H.G., Ji, S.H., Ji, M., An, Y.L., 2008. Inorg. Chem. 47, 3922–3924.
Kong, R.M., Zhang, X.B., Zhang, L.L., Jin, X.Y., Huan, S.Y., Shen, G.L., Yu, R.Q., 2009. Chem. Commun., 5633–5635.
Lao, R.J., Song, S.P., Wu, H.P., Wang, L.H., Zhang, Z.Z., He, L., Fan, C.H., 2005. Anal. Chem. 77, 6475–6480.
Li, F., Feng, Y., Liu, S., Tang, B., 2011. Chem. Commun. 47, 6347–6349.
Liu, S.J., Nie, H.G., Jiang, J.H., Shen, G.L., Yu, R.Q., 2009. Anal. Chem. 81, 5724–5730.
Miyake, Y., Togashi, H., Tashiro, M., Yamaguchi, H., Oda, S., Kudo, M., Tanaka, Y., Kondo, Y., Sawa, R., Fujimoto, T., Machinami, T., Ono, A., 2006. J. Am. Chem. Soc. 128, 2172–2173.
Morel, F.M.M., Kraepiel, A.M.L., Amyot, M., 1998. Annu. Rev. Ecol. Syst. 29, 543–566.
Morita, M., Yoshinaga, J., Edmonds, J.S., 1998. Pure Appl. Chem. 70, 1585–1615.
Mor-Piperberg, G., Tel-Vered, R., Elbaz, J., Willner, I., 2010. J. Am. Chem. Soc. 132, 6878–6879.
Niu, X., Ding, Y., Chen, C., Zhao, H., Lan, M., 2011. Sens. Actuators B Chem. 158, 383–387.
Nolan, E.M., Lippard, S.J., 2008. Chem. Rev. 108, 3443–3480.
Nolan, M.A., Kounaves, S.P., 1999. Anal. Chem. 71, 3567–3573.
Park, H., Hwang, S.J., Kim, K., 2012. Electrochem. Commun. 24, 100–103.
Ruys, D.P., Andrade, J.F., Guimaraes, O.M., 2000. Anal. Chim. Acta. 404, 95–100.
Shi, L., Chu, Z., Dong, X., Jin, W., Dempsey, E., 2013a. Nanoscale 5, 10219–10225.
Shi, L., Chu, Z., Liu, Y., Jin, W., Chen, X., 2013b. Biosen. Bioelectron. 49, 184–191.
Steel, A.B., Herne, T.M., Tarlov, M.J., 1998. Anal. Chem. 70, 4670–4677.
Tanaka, Y., Yamaguchi, H., Oda, S., Kondo, Y., Nomura, M., Kojima, C., Ono, A., 2006. Nucleosides, Nucleotides Nucleic Acids 25, 613–624.
Tong, P., Zhang, L., Xu, J.J., Chen, H.Y., 2011. Biosen. Bioelectron. 29, 97–101.
Wang, J., Liu, G.D., Merkoci, A., 2003. J. Am. Chem. Soc. 125, 3214–3215.
Wang, G., Huang, H., Zhang, X., Wang, L., 2012. Biosens. Bioelectron. 35, 108–114.
Wang, M., Feng, W., Shi, J., Zhang, F., Wang, B., Zhu, M., Li, B., Zhao, Y., Chai, Z., 2007. Talanta 71, 2034–2039.
Yang, L., Kinoshita, S., Yamada, T., Kanda, S., Kitagawa, H., Tokunaga, M., Ishimoto, T., Ogura, T., Nagumo, R., Miyamoto, A., Koyama, M., 2010. Angew. Chem.-Int. Ed. 49, 5348–5351.
Yuan, T., Liu, Z., Hu, L., Zhang, L., Xu, G., 2011. Chem. Commun. 47, 11951–11953.
Zhang, J., Song, S., Wang, L., Pan, D., Fan, C., 2007. Nat. Protoc. 2, 2888–2895.
Zhang, J., Song, S.P., Zhang, L.Y., Wang, L.H., Wu, H.P., Pan, D., Fan, C.H., 2006. J. Am. Chem. Soc. 128, 8575–8580.
Zhuang, J., Fu, L., Tang, D., Xu, M., Chen, G., Yang, H., 2013. Biosen. Bioelectron. 39, 315–319.